



## The role of residue Thr122 of methylamine dehydrogenase on the proton transfer from the iminoquinone intermediate to residue Asp76

Gustavo Pierdominici-Sottile<sup>a</sup>, Marcelo A. Martí<sup>b</sup>, Juliana Palma<sup>a,\*</sup>

<sup>a</sup>Centro de Estudios e Investigaciones, Universidad Nacional de Quilmes, Sáenz Peña 352, B1876BXD Bernal, Argentina

<sup>b</sup>Departamento de Química Inorgánica, Analítica y Química-Física, INQUIMAE-CONICET, Facultad de Ciencias Exactas y Naturales, Universidad de Buenos Aires, Ciudad Universitaria, Pabellón 2, C1428EHA Buenos Aires, Argentina

### ARTICLE INFO

#### Article history:

Received 31 July 2007

In final form 13 March 2008

Available online 17 March 2008

### ABSTRACT

We present the results of combined molecular dynamics and full-quantum calculations aimed at elucidating the role of residue Thr122 of the enzyme methylamine dehydrogenase. Calculations were performed on the native structure and the T122A mutant. We found that the presence of Thr122 has a deleterious effect on the proton transfer step that is proposed to determine the rate of the reaction. Besides, at the PM3 level, the substitution of Thr122 by Ala does not significantly modify the preference of the proton by atom OD2 of Asp76. Transmission coefficients obtained from MP2/6-31G(d,p)//PBE/DZP minimum energy paths show that proton tunneling is significant.

© 2008 Elsevier B.V. All rights reserved.

### 1. Introduction

Methylamine dehydrogenase catalyzes the oxidation of methylamine to formaldehyde and ammonia. The reaction involves a proton transfer from the methyl group of the substrate to an active site base [1]. This step presents an expanded kinetic isotopic effect which is temperature independent [2]. However, the rate constants are temperature dependent. The step has been the subject of several theoretical studies [3–11].

Davidson and co-workers performed site-directed mutagenesis experiments to determine the role of polar residues of the active site in catalysis. However, this role could not be assessed as mutations that removed the reactive oxygen atoms of these residues resulted in very low levels of MADH production [12]. Fig. 1 shows a model of the active site with the cofactor, TTQ [1], in the iminoquinone form. Residue numbers correspond to those found in MADH from *Paracoccus denitrificans* (PDB entry 2BBK) [13]. It is now accepted that Asp76 is the base that participates in the proton transfer step [8,14]. Besides, Davidson has demonstrated that this residue is involved in the biogenesis of the cofactor [15]. The role of Thr122 is still unclear.

Quantum calculations on active site models established that the presence of Thr122 increases the barrier for the transference [8]. This detrimental effect can be rationalized considering that Thr122 forms an H-bond with Asp76 and therefore withdraws electron density from it. Later on, molecular dynamics simulations showed that this H-bond restricts the rotation of the  $-\text{CO}_2^-$  group [8]. Thus, Thr122 could facilitate the reaction by holding the car-

boxylic group in an appropriate orientation for the transference. As the energy strongly depends on this orientation, it is not clear which of the two effects is the most important. Thr122 could also determine which oxygen atom (OD1 or OD2) is the most probable acceptor. Recent studies have noticed this and have indicated that Thr122 could have a role in modulating tunnelling probabilities [10,11].

### 2. Computational details

We combined molecular dynamics (MD) simulations of the enzyme with full-quantum (QM) calculations of the active site model of Fig. 1. In one set of computations we used the structure of the native enzyme; in another set we used the structure obtained by replacing Thr122 with Ala. Finally, with the data corresponding to the wild type form, we estimated the transmission coefficients for proton transfer to each oxygen atom of Asp76.

The MD simulations were done with AMBER7 [16], using the AMBER96 force field and the parameters for TTQ that were presented elsewhere [9]. The protocol used to prepare and equilibrate the structures is the same as described in Ref. [9]. The production stage at 300 K and 1 atm lasted for 900 ps. Configurations were sampled every 1.0 ps. The simulation of the T122A mutant was extended up to 5.0 ns to check its stability. The analysis of the energies, temperature, pressure and RMSD showed that the structure remains stable (see Fig. 2). This *in silico* stability enabled us to compare the dynamics of the two structures. Nevertheless, we acknowledge that this fact does not preclude the idea that Thr122 could be necessary to keep the enzyme in its folded state. The unfolding process could take much longer times than the ones analyzed here.

\* Corresponding author. Fax: +54 11 4365 7182.

E-mail address: [juliana@unq.edu.ar](mailto:juliana@unq.edu.ar) (J. Palma).

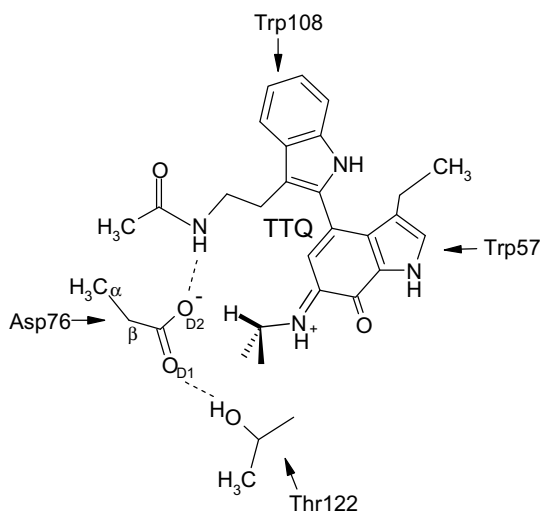


Fig. 1. Model of the active site used in the QM calculations. Note that each  $C_{\alpha}$  atom was replaced with a  $-CH_3$  group.

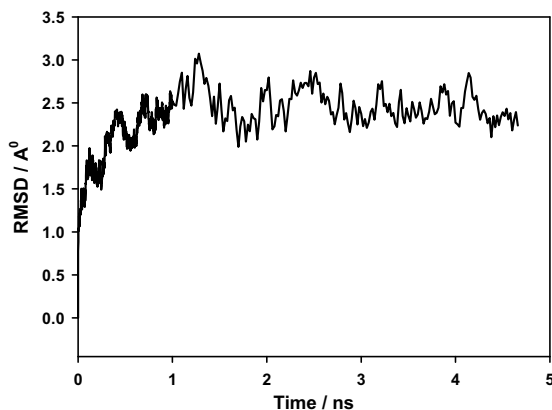


Fig. 2. RMSD for the MD simulation of the T122A mutant.

Full-QM computations, performed with GAUSSIAN 98 [17], were used to calculate the potential energy curves for the instantaneous proton transfer, for structures sampled from the MD simulations. From each structure, we cut the model shown in Fig. 1. Then, we stretched the C–H bond from 1.0 Å to 2.8 Å in 19 steps and performed single-point QM calculations at every step. During this process, the rest of the atoms were kept in their initial positions. These calculations were done at the PM3 level of theory.

Each curve was analyzed to see whether it had a double minimum or not. Curves that did not show a double minimum were labelled as *non-reactive*. On the contrary, curves with a double minimum were labelled as *reactive*, even though the barrier were so high or the reaction so endothermic as to render the transference very unlikely. The curves labelled as *reactive* were analyzed to calculate the barrier for the transference and to see whether the proton acceptor was atom OD1 or OD2. For the wild type form we also evaluated the interaction energy,  $E_{\text{int}}^z$ , between Thr122 and the reactive centre (Asp76 + TTQ):

$$E_{\text{int}}^z = E^z(\text{Asp76} + \text{TTQ} + \text{Thr122}) - E^z(\text{Asp76} + \text{TTQ}) - E^z(\text{Thr122}).$$

Here  $E^z(\text{Asp76} + \text{TTQ} + \text{Thr122})$  is the energy of the whole active site model, while  $E^z(\text{Asp76} + \text{TTQ})$  and  $E^z(\text{Thr122})$  are the energies of the isolated subsystems. The superscript  $z$  indicates whether the structure corresponds to reactants or products.

Full-QM computations were also used to determine the minimum energy paths (MEPs) for the model of Fig. 1. These calculations were done with the SIESTA code [18] at a DFT level of theory, with the PBE functional and a double zeta plus polarization basis set. The structure of the model in the reactants configuration was minimized by fixing the position of each  $C_{\alpha}$  atom, to simulate the restrictions imposed by the protein backbone. Then, the term  $V(\xi) = k(\xi - \xi_0)^2$  was added to the potential, where  $\xi$  is the reaction coordinate and  $\xi_0$  is the desired value of the reaction coordinate. The system was forced to follow the MEP by varying  $\xi_0$ . We set  $k = 200.0$  kcal/mol and defined  $\xi = d_{\text{CH}} - d_{\text{OH}}$ , where  $d_{\text{CH}}(d_{\text{OH}})$  is the length of the bond being broken(formed). Finally, the energies were recalculated at the B3LYP/6-31 G(d,p) and MP2/6-31G(d,p) levels of theory, using GAUSSIAN 98.

The transmission coefficients were calculated using the Hamiltonian:

$$\hat{H} = -\frac{\hbar^2}{2m_{\text{eff}}} \frac{\partial^2}{\partial \xi^2} + V^{\text{MEP}}(\xi)$$

Here  $m_{\text{eff}}$  is the mass of the proton divided by 4.0 and  $V^{\text{MEP}}(\xi)$  gives the energy along the MEP. The factor of 1/4 in  $m_{\text{eff}}$  arises because  $\hat{H}$  is expressed in terms of the reaction coordinate instead of the proton coordinate. We used the formula proposed by Miller [19]:

$$\kappa(T) = \frac{k(T)}{k(T)_{\text{TST,CL}}} = 2\pi\beta e^{\beta V_0^{\ddagger}} \int_0^{\infty} C_{\text{ff}}(T) dt.$$

Here  $C_{\text{ff}}(T)$  is the flux–flux autocorrelation function,

$$C_{\text{ff}}(T) = \sum_{m=1}^2 f_m \langle u_m(t) | \hat{F} | u_m(t) \rangle,$$

$f_m$  and  $|u_m\rangle$  are the eigenvalues and eigenfunctions, respectively, of the boltzmanized flux operator  $\hat{F}_{\beta} = e^{-\beta\hat{H}/2} \hat{F} e^{-\beta\hat{H}/2}$ ,  $\hat{F} = [\hat{H}, h]$  and  $h$  is the Heaviside function. To determine  $f_m$  and  $|u_m\rangle$  we diagonalized the representation of  $\hat{F}_{\beta}$  in the basis set of the eigenfunctions of  $\hat{H}$ . The eigenfunctions of  $\hat{H}$  were obtained using a particle-in-a-box DVR basis set. Because  $|u_m\rangle$  was expressed as a linear combination of eigenfunctions of  $\hat{H}$ , the functions  $|u_m(t)\rangle$  were evaluated by direct application of the evolution operator. We used 100 DVR functions, expanding a range of  $12.0a_0$  centred at the maximum of the MEP. Only eigenfunctions of  $\hat{H}$  with eigenvalues  $<55.0$  kcal/mol above the bottom of the reactants well were used in the expansion. To avoid recrossings, the energy profiles were modified by setting  $E = E_{\text{min}}^{\text{react}}$  for  $r \leq r_{\text{min}}^{\text{react}}$  and  $E = E_{\text{min}}^{\text{prod}}$  for  $r \geq r_{\text{min}}^{\text{prod}}$ , where  $r_{\text{min}}^{\text{react}}$  ( $r_{\text{min}}^{\text{prod}}$ ) indicates the location of the reactants (products) well. Metiu and co-workers have demonstrated that this approximation is similar to conventional (i.e. not variational) TST [20]. The temperature was set to 300 K.

### 3. Results and discussion

MD simulations confirm that replacing Thr122 with Ala gives greater mobility to the carboxylic group of Asp76. For example, the probability distribution for the  $C_{\alpha}$ – $C_{\beta}$ – $C$ – $O_{\text{OD1}}$  torsion shows a broader distribution in the simulation of the mutant. The standard deviations are  $\sigma = 17.3^\circ$  for the mutant and  $\sigma = 12.0^\circ$  for the wild type form. Another indication of this greater mobility is that the hydrogen bond between OD2 and Trp108 is weakened. This H-bond appears in 32.2% of the structures of the wild type form, but only 8.4% of the structures of the mutant.

The mutation has only a moderate effect on the H-bonds between the methyl group of the substrate and Asp76. The H-bond with OD2 is present in 34.3% of the structures of the wild type form and 38.0% of the structures of the mutant. For OD1 the figures are 18.8% (wild type) and 14.1% (mutant). Thus, in both cases, the H-bond with OD2 is significantly more likely than the H-bond with

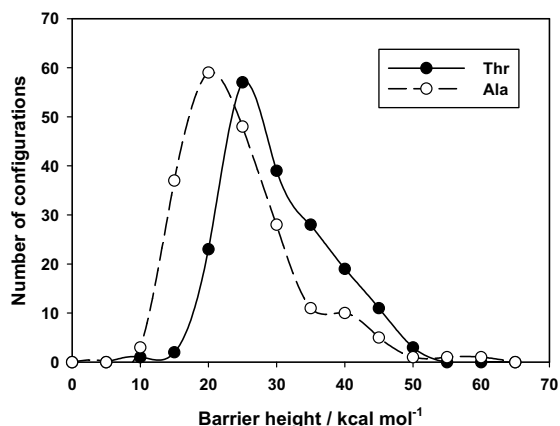


**Fig. 3.** Distribution of the PM3 instantaneous barriers corresponding to proton transfer to OD2. Black circles are used for the wild type form and white circles for the T122A mutant.

OD1, but the preference is somewhat smaller for the wild type form.

We found 208 (23.1%) *reactive* curves for the wild type form and 234 (26.0%) for the T122A mutant. Atom OD2 was the acceptor of the proton in 88.0% of the *reactive* cases of the wild type form and 87.2% of the mutant. The average values for the barriers were  $27.6 \pm 7.6$  kcal/mol (wild type) and  $22.0 \pm 8.3$  kcal/mol (mutant). Fig. 3 shows the probability distributions for the barriers. The distribution of the mutant is clearly shifted to lower energies than that corresponding to the native form. Similar results were obtained for the transference to OD1. In that case the average barriers were  $27.5 \pm 8.8$  kcal/mol (wild type) and  $21.8 \pm 9.0$  kcal/mol (mutant). These results show that the transfer is favoured when Thr122 is replaced with Ala: there are more *reactive* configurations and they show significantly lower barriers. The results also suggest that the replacement of Thr122 by Ala does not modify the preference of the proton by atom OD2.

The instantaneous barriers vary within a broad range. Moreover, for many structures it is not even possible to calculate a barrier, as the energy just increases when the C–H bond is stretched (these are the *non-reactive* curves). This happens because all the atoms, except the proton being transferred, were fixed during the calculations. Having a relatively small barrier requires an appropriate orientation between the donor and the acceptor. It also requires that, when the proton is transferred, the –COOH group adopts an appropriate configuration. Similar and even larger variations have been reported for other enzymatic reactions [21].

The values of  $E_{\text{int}}^z$  are plotted in Fig. 4. For both transferences, Thr122 has a more favourable interaction with the structures corresponding to reactants than with the ones corresponding to products. For OD2, Thr122 has a stabilizing interaction in all the structures of reactants and 65.5% of the structures of products. The average interaction energies are  $-8.1$  kcal/mol (reactants) and  $-0.9$  kcal/mol (products). For OD1, the interaction is stabilizing in nearly all the structures of reactants, but it is destabilizing in all the structures of products. The average interaction energies are  $-6.2$  kcal/mol (reactants) and  $+6.9$  kcal/mol (products). These results agree with the ones of Ranaghan et al. [11] at indicating that the interaction with Thr122 is more favourable for reactants than for products. The agreement is significant considering the differences in the methodologies used in each study. However, our energies are higher than those of reference [11]. The differences can be explained considering that the values reported in reference [11] correspond to the MEP, while the ones presented here correspond to the instantaneous profiles. Thus, for example, Ranaghan

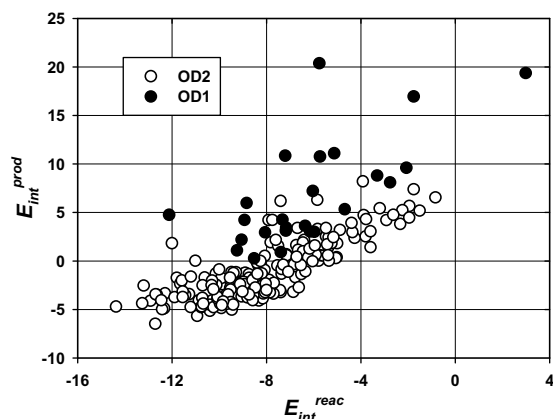


**Fig. 4.** Interaction energies between residue Thr122 and the reactive centre (Asp76 + TTQ).  $E_{\text{int}}^{\text{react}}$  ( $E_{\text{int}}^{\text{prod}}$ ) corresponds to the interaction at the reactants (products) well.

et al. observed that the hydroxyl group of Thr122 rotates away from Asp76 as the proton is transferred towards OD1. In our calculations, the residue is frozen and therefore the energy increases with the transference. Núñez et al. [10] also evaluated the effect of Thr122 and found that the residue mainly stabilizes the products. In those QM/MM calculations the MEPs were determined relaxing the geometry of the quantum subsystem while fixing the geometry of the classical subsystem (which included residue Thr122). As Ranaghan et al. discussed in reference [11] this treatment would be the origin of the stabilizing effect reported by Núñez et al.

The barriers along the MEPs are displayed in Table 1. Different levels of theory agree at indicating that the barriers become lower when Thr122 is replaced with Ala. Thus, the deleterious effect of Thr122 is not eliminated by relaxing the structures. Table 2 shows structural details of the MEPs. Good agreement is found between the distances of Table 2 and those reported elsewhere [11], with the exception of  $d(\text{C}-\text{OD1})$  and  $d(\text{H}-\text{OD1})$  at the reactants configuration. In these cases we got somewhat higher values. Finally, we note that the B3LYP/6-31G(d,p)//PBE/DZP barrier for the wild type form is similar to the B3LYP/6-31G(d)//PM3 barriers reported elsewhere [8].

In Fig. 5 we show the  $C_{\text{tr}}(t)$ s obtained from the MEPs determined at the MP2/6-31G(d,p)//PBE/DZP level. The corresponding transmission coefficients are 272.3 for transfer to OD2 and 62.2 for transfer to OD1. At the B3LYP/6-31G(d,p)//PBE/DZP level, the transmission coefficients are 18.9 for OD2 and 4.5 for OD1.

**Table 1**  
Barriers in kcal/mol along to the MEPs

|       | OD2  |      | OD1  |       |
|-------|------|------|------|-------|
|       | Ala  | Thr  | Ala  | Thr   |
| B3LYP | 3.39 | 7.86 | 1.82 | 7.31  |
| MP2   | 4.01 | 8.46 | 4.26 | 10.71 |

**Table 2**  
Main distances at the MEPs

| Distance | OD2        |            | OD1        |            |
|----------|------------|------------|------------|------------|
|          | Reactants  | TS         | Reactants  | TS         |
| C–H      | 1.14(1.14) | 1.42(1.32) | 1.14(1.14) | 1.33(1.14) |
| C–O      | 2.96(3.02) | 2.63(2.63) | 3.07(3.24) | 2.61(2.91) |
| H–O      | 1.82(1.87) | 1.21(1.31) | 2.48(2.49) | 1.28(1.88) |

Values within parenthesis correspond to the mutant.

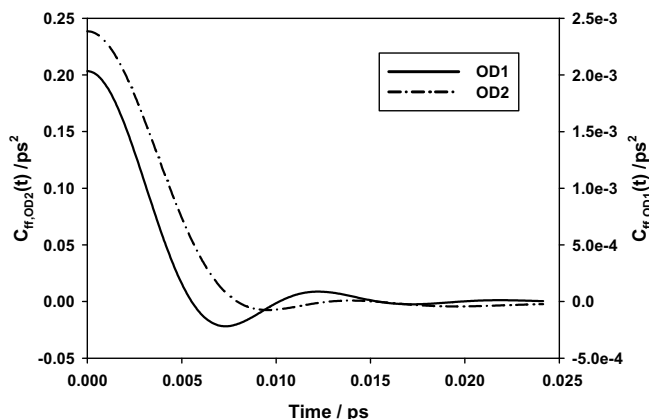


Fig. 5. Flux–flux autocorrelation functions for the MP2/6-31G(d,p)//PBE/DZP MEPs. Note that  $C_{fr,OD1}(t)$  and  $C_{fr,OD2}(t)$  are plot on different scales.

Observed differences are attributed to B3LYP barriers being lower than the MP2 ones, and also to the transfer being exothermic in MP2 calculations ( $\Delta E = -1.30$  kcal/mol for OD1 and  $-1.83$  kcal/mol for OD2), but endothermic in B3LYP calculations ( $\Delta E = 0.52$  kcal/mol for OD1 and  $1.83$  kcal/mol for OD2).

The fact that  $\kappa(T)$  is larger for OD2 than OD1 can be explained noting that the OD1 barrier is wider. To verify this, we adjusted the MP2 MEPs with the functional form proposed by Ahmed [22]:

$$V(x) = V_0 \left( 1 - \left( \frac{1 - \exp(x/a)}{1 + c \exp(x/a)} \right)^2 \right).$$

The parameters were  $a = 0.5128$ ,  $c = 0.9337$  and  $V_0 = 0.0170$  for OD1 and  $a = 0.3525$ ,  $c = 0.9036$  and  $V_0 = 0.0135$  for OD2 (all in atomic units). It should be noted that the barriers in the original and the fitted curves are exactly the same. Using the analytical expression for the microcanonical transmission coefficient given by Ahmed [22] we calculated the corresponding  $\kappa(T)$ . We obtained  $\kappa(T) = 81$  for OD1 and  $\kappa(T) = 319$  for OD2. These values are similar to the ones evaluated from the original curves. On the other hand, the transmission coefficients calculated by applying the flux–flux autocorrelation function formalism on the fitted curves are 76 for OD1 and 303 for OD2, in good agreement with the values obtained using the formulas of Ref. [22].

Results presented here agree with previous calculations at indicating that tunnelling is significant for this transference. However,

recent reports indicate that the effect is more important for OD1 than OD2 [10,11]. Differences between those results and ours can be attributed to the use of different levels of theory to calculate the MEPs. One should also note that the MEPs presented here were obtained with an active site model. Considering the effect of the whole protein environment could make the barriers somewhat higher, but also the  $\Delta E$  more endothermic [11]. As these variations tend to compensate to each other, it is not easy to predict their impact on the transmission coefficients.

Summarizing: combined MD + QM computations indicate that the presence of Thr122, a residue that is 100% conserved in MADH, is detrimental for the proton transfer step that determines the rate of the catalyzed reaction. Besides, at the PM3 level, the absence of Thr122 does not modify the preference of the proton by atom OD2 of Asp76. Transmission coefficients obtained from the PM2/6-31G(d,p)//PBE/DZP MEPs indicate that the contribution of tunneling is significant and is more important in the transfer to OD2 than OD1.

## References

- [1] H.B. Brooks, L.H. Jones, V.L. Davidson, *Biochemistry* 32 (1993) 2725.
- [2] J. Basran, M.J. Sutcliffe, N.S. Scrutton, *Biochemistry* 38 (1999) 3218.
- [3] G. Tresadern, J.P. Mcnamara, M. Mohr, H. Wang, N.A. Burton, I.H. Hillier, *Chem. Phys. Lett.* 358 (2002) 489.
- [4] C. Alhambra, M.L. Sanchez, J.C. Corchado, J. Gao, D.G. Truhlar, *Chem. Phys. Lett.* 355 (2002) 388.
- [5] G. Tresadern, H. Wang, P.F. Faulder, N.A. Burton, I.H. Hillier, *Mol. Phys.* 101 (2003) 2775.
- [6] J.S. Mincer, S.D. Schwartz, *J. Chem. Phys.* 120 (2004) 7755.
- [7] W. Siebrand, Z. Smedarchina, *J. Phys. Chem. B* 108 (2004) 4185.
- [8] G. Pierdominici-Sottile, J. Echave, J. Palma, *Int. J. Quantum Chem.* 105 (2005) 937.
- [9] G. Pierdominici-Sottile, J. Echave, J. Palma, *J. Phys. Chem. B* 110 (2006) 11592.
- [10] S. Nuñez, G. Tresadern, I.H. Hillier, N.A. Burton, *Philos. Trans. R. Soc. London Ser. B* 361 (2006) 1387.
- [11] K.E. Ranaghan, L. Masgrau, N.S. Scrutton, M.J. Sutcliffe, A.J. Mulholland, *Chem. Phys. Chem.* 8 (2007) 1816.
- [12] D.P. Sun, L.H. Jones, F.S. Mathews, V.L. Davidson, *Protein Eng.* 14 (2001) 675.
- [13] L.Y. Chen, N. Doi, R.C.E. Durley, A.Y. Chistoserdov, M.E. Lidstrom, V.L. Davidson, F.S. Mathews, *J. Mol. Biol.* 276 (1998) 131.
- [14] V.L. Davidson, Z.Y. Zhu, *J. Mol. Catal. B-Enzym.* 8 (2000) 69.
- [15] L.H. Jones, A.R. Pearson, Y. Tang, C.M. Wilmot, V.L. Davidson, *J. Biol. Chem.* 280 (2005) 17392.
- [16] D.A. Case et al., *AMBER7*, University of California, San Francisco, 2002.
- [17] M.J. Frisch et al., *Gaussian Inc.*, Pittsburg, PA, 1998.
- [18] J.M. Soler, E. Artacho, J.D. Gale, A. García, J. Junquera, P. Ordejón, D. Sánchez-Portal, *J. Phys.: Condens. Matter* 14 (2002) 2745.
- [19] H.B. Wang, X. Sun, W.H. Miller, *J. Chem. Phys.* 108 (1998) 9726.
- [20] G. Wahnstrom, B. Carmeli, H. Metiu, *J. Chem. Phys.* 88 (1988) 2478.
- [21] V. Guallar, D.L. Harris, V.S. Batista, W.H. Miller, *J. Am. Chem. Soc.* 124 (2002) 1430.
- [22] Z. Ahmed, *Phys. Rev. A* 47 (1993) 4761.